Inorg. Chem. **2006**, *45*, 10457−10466

Synthesis of Isostructural Cage Complexes of Copper with Cobalt and Nickel for Deposition of Mixed Ceramic Oxide Materials

Mazhar Hamid,[†] Asif A. Tahir,[†] Muhammad Mazhar,*[,†] Matthias Zeller,[‡] Kieran C. Molloy,[§] and Allen D. Hunter[‡]

Department of Chemistry, Quaid-I-Azam University, Islamabad 45320, Pakistan, STaRBURSTT Cyberdiffraction Consortium and Department of Chemistry, Youngstown State University, 1 University Plaza, Youngstown, Ohio 44555-3663, and Department of Chemistry, University of Bath, Claverton Down, Bath, BA2 7AY U.K.

Received January 20, 2006

Heterobimetallic molecular precursors $[Co_2(acac)_2(\mu\text{-}OH)_2Cu_4(dmae)_4Cl_4]$ (**2**) and $[Ni_2(acac)_2(\mu\text{-}OH)_2Cu_4(dmae)_4Cl_4]$ (**3**) [dmaeH = *N*,*N*-dimethylaminoethanol and acac = 2,4-pentanedionate] for the deposition of mixed oxide thin films were prepared by the interaction of tetrameric *N*,*N*-dimethylaminoethanolato copper(II) chloride, $[Cu(dmae)Cl]_4$ (**1**) with $M(acac)_2 \cdot xH_2O$, [M = Co, Ni] in toluene. Both heterobimetallic cage complexes were characterized by melting point, elemental analysis, FT-IR spectroscopy, mass spectrometry, magnetometery, and single-crystal X-ray diffraction. Complexes **2** and **3** are isostructural and crystallize in the monoclinic space group $P2_1/n$. A TGA study shows that both complexes undergo controlled thermal decomposition at 450 °C to give mixed metal oxides. Solid-state infrared spectroscopy (FT-IR), scanning electron microscopy (SEM), energy-dispersive X-ray analysis (EDX), and X-ray powder diffraction (XRD) analysis were performed to analyze the chemical composition and surface morphology of the deposited oxide thin films. The results obtained indicate the formation of impurity-free crystalline mixed oxide films with particle sizes ranging from 0.55 to 2.0 μm.

Introduction

Within about the last two decades, the development of modern technologies with their appeal for miniaturization and increased performance has promoted the search for alternative ways to produce materials that are capable of meeting new demands. For ceramic materials, the traditional methods were based mainly on reactions in the solid state, and often, control over the composition, structure, and morphology of the materials obtained was rather limited, thus encouraging the search for more rational and custom-tailored methods. A broad variety of newly developed synthetic procedures now allows desired products to be obtained under mild conditions; these methods are commonly known as the *Soft Chemistry Approach*.[1−3] The majority of these techniques, such as Sol−Gel technology, metal−organic chemical vapor deposition (MOCVD), metal−organic deposition (MOD), and others, involve the utilization of organometallic compounds or metal complexes with organic ligands, such as alkoxides, β-diketonates, carboxylates, etc. These metal complexes, all of which can be easily hydrolytically or thermally decomposed, are usually referred to as the molecular precursors. Single-source precursors (SSP) with molecules containing all the necessary elements required by the final material in the proper ratio have proven extremely versatile since they often decompose cleanly under mild conditions in a controllable manner.[4,5]

An additional improvement was provided by single-source bimetallic compounds, which are capable of delivering both metallic elements of a desired material simultaneously, thus generating a complex ceramic material in a single step and removing the problems resulting from the use of a multi-

* To whom correspondence should be addressed. E-mail mazhar42pk@yahoo.com.
[†] Quaid-I-Azam University.
[‡] Youngstown State University.
[§] University of Bath.

(1) (a) Hubert-Pfalzgraf, L. G. *Coord. Chem. Rev.* **1998**, *180*, 967−997. (b) Hubert-Pfalzgraf, L. G. *Inorg. Chem. Commun.* **2003**, *6*, 102−120 and references therein. (c) Hubert-Pfalzgraf, L. G. *New J. Chem.* **1995**, *19*, 727−730.
(2) Corriu, R. *J. Organomet. Chem.* **2003**, *686*, 32−41. (b) Corriu, R. *Eur. J. Inorg. Chem.* **2001**, 1109−1121.
(3) Rao, C. N. R.; Cheetham, A. K. *J. Mater. Chem.* **2001**, *11*, 2887−2894.
(4) Veith, M. *Dalton Trans.* **2002**, 2405−2412.
(5) Kessler, V. G. *Chem. Commun.* **2003**, 1213−1222.

10.1021/ic060119u CCC: $33.50
Published on Web 11/18/2006

component precursor mixture such as matching of volatilities and decomposition temperatures, etc.[6]

Mixed-metal oxides and their thin films exist in a variety of compositions and crystal structures and their physical and electrical properties vary widely, leading to a vast range of potential applications[7,8] in advanced materials technology, such as "electroceramic" oxides. They have important applications in the fields of microelectronics and telecommunications, such as next-generation computer memories, fuel cells, gate dielectric layers, infrared detectors, optical waveguides, and electrooptic storage. However, the most common use for mixed-metal oxides and alloys has been in the area of industrial effluent and waste treatment and in catalysis, where they are used as the catalyst, as a cocatalyst, or as catalyst supports.[9,10] Specifically, aluminum-containing mixed-metal oxides have many applications in this field,[11−13] as do cobalt- and copper-based mixed-metal oxide catalysts for the oxidation of CO by O_2,[14] for the conversion of synthesis gas ($CO/CO_2/H_2$) to higher alcohols,[15,16] and for the Fischer−Tropsch synthesis[17] (because of their attractive properties, such as stability, high activity at low pressure, and selectivity).

The advent of superconducting and catalytic properties in ternary metal oxide systems has promoted a growing interest in the synthesis and characterization of simple Cu-containing alkoxides[18,19] as well as heterobimetallic alkoxide components $MM'(OR)_{x-y}$ with precise stoichiometries,[20] but rapid progress in this field has been slowed by a series of obstacles. The synthesis of simple, soluble metal aminoalkoxides based on ligands such as *N*,*N*-dimethylaminoethanol (dmaeH) leads to a preferential formation of mononuclear alkoxides.[21,22] Furthermore, conventional copper alkoxides usually exhibit an extensive association via μ-alkoxide bridges between two or more metal centers and thus form mostly insoluble and nonvolatile species.[23] For some homometallic alkoxides, the solubility has been improved by the use of chelating or sterically crowded ligands, which because of their multidentate behavior or steric bulk are able to reduce the association of the metal alkoxides to produce soluble derivatives.[24]

Recently, many researchers started extensive work on the development of heterobimetallic precursors of copper with main group and transition metals for the deposition of metal oxides. Typical examples are complexes such as $[Cu_2Co^{II}Co^{III}_2(OCMe)_4(Htea)_2(tea)_2]_2\cdot(HOMe)$,[25] $[Cu(Me_6Cy)][Ni(CN)_4]$,[26] $[Cu(L)(H_2O)Ni(hfa)_2(H_2O)]$,[27] $[(CuL^1)Ni(pmtn)(NCS)]ClO_4$, $[Cu(L^2)Ni(pmtn)(NCS)]ClO_4$, $[(CuL^3)Ni(pmtn)(NCS)]ClO_4$,[28] $[Ni(H_2L)_2][CoCu(L)_2(H_2L)(NCS)]_2\cdot(NCS)_2$, $[Ni(H_2L)_2][CuCo(L)_2(H_2L)(NCS)]_2Br_2\cdot 2H_2O$, $[CuCoCd(H_2L)_2(L)_2(NCS)Br_2]\cdot CH_3OH$,[29] and $[Cu(L)Co(bpy)_2(ClO_4)_2\cdot 0.5C_2H_5OH\cdot H_2O$,[30] but none of these compounds has been investigated for its properties as a precursor for chemical vapor deposition. The heterometallic complex $[Co_2Ni_2(acac)_4(\mu_3\text{-}OMe)_4(OAc)_2]$[31] has, however, been used to prepare zeolite-supported oxide catalysts, and it exhibited extremely high activity toward the oxidation of methanol.

Following our work directed toward the design of heterobimetallic complexes for mixed-metal oxides and taking advantage of the chelating character of aminoalcohol ligands such dmaeH with the possibility of generating high-nuclearity species,[32−34] we have reacted copper(II) methoxy chloride with dmaeH to synthesize tetrameric *N*,*N*-dimethylaminoethanolato copper(II) chloride (**1**). The reaction of $[Cu(dmae)Cl]_4$ (**1**) with $M(acac)_2\cdot xH_2O$ [M = Co, Ni; acac = 2,4-pentanedionate] gives the heterobimetallic complexes $Co_2(acac)_2(\mu\text{-}OH)_2Cu_4(dmae)_4Cl_4$ (**2**) and $Ni_2(acac)_2(\mu\text{-}OH)_2Cu_4(dmae)_4Cl_4$ (**3**). Here we report the synthesis and

(6) Jones, A. C. *J. Mater. Chem.* **2002**, *12*, 2576−2590.
(7) Auciello, O., Ramesh, R., Eds. Special Issue on Electroceramic Thin Films, Parts I and II. *MRS Bull.* **1996**, *21* (6, 7), and references therein.
(8) Jones, A. C.; Leedham, T. J.; Wright, P. J.; Crosbie, M. J.; Lane, P. A.; Williams, D. J.; Fleeting, K. A.; Otway D. J.; O'Brien, P. *Chem. Vap. Deposition* **1998**, *4*, 46−49.
(9) Amigo, R.; Asenjo, J.; Krotenko, E.; Torres, F.; Tejada, J. *Chem. Mater.* **2000**, *12*, 573−579.
(10) Rodriguez, J. A.; Hanson, J. C.; Chaturvedi, S.; Maiti, A.; Brito, J. L. *J. Chem. Phys.* **2000**, *112*, 935−945.
(11) Heinz, D.; Hoelderich, W. F.; Krill, S.; Boeck, W.; Huthmacher, K. *J. Catal.* **2000**, *192*, 1−10.
(12) Kiessling, D.; Went, G.; Hagenau, K.; Schoellner, R. *Appl. Catal.* **1991**, *71*, 69−78. (b) Watanabe, H.; Koyasu, Y. *Appl. Catal., A* **2000**, 194−195, 479−485.
(13) (a) Corma, A. *Chem. Rev.* **1995**, *95*, 559−614. (b) Reddy, B. N.; Subrahmanyam, M. *Langmuir* **1992**, *8*, 2072−2073.
(14) Angelov, S.; Mehandjiev, D.; Piperov, B.; Zarkov, V.; Terlecki-Baricevic, A.; Jovanovic, D.; Jovanovic, Z. *Appl. Catal.* **1985**, *16*, 431−437.
(15) (a) Fujimoto, K.; Oba, T. *Appl. Catal.* **1985**, *13*, 289−293. (b) Xiaoding, X.; Doesburg, E. B. M.; Sholten, J. J. F. *Catal. Today* **1987**, *2*, 125−170. (c) Baker, J. E.; Burch, R.; Golunski, S. E. *Appl. Catal.* **1989**, *53*, 279−297 and references therein.
(16) Sugier, A.; Freund, E. US Patent 4122110, 1978.
(17) Fornasari, G.; Gusi, S.; Trifir, F.; Vaccari, A. *Ind. Eng. Chem. Res.* **1987**, *26*, 1500−1505 and references therein.
(18) Bednorz, J. G.; Muller, K. A.; Takashige, M. *Science* **1987**, *236*, 73−79.
(19) Edwerds, P. P.; Harrison, M. R.; Jones, R. *Chem. Ber.* **1987**, *23*, 962−965.
(20) Vieth, M.; Mathur, S.; Huch, V. *J. Am. Chem. Soc.* **1996**, *118*, 903−904.
(21) Chi, Y.; Ranjan, S.; Chou, T.-Y.; Liu, C.-S.; Peng, S.-M.; Lee, G.-H. *J. Chem. Soc., Dalton Trans.* **2001**, 2462−2466.
(22) Breeze, R. S.; Wang, S. *Inorg. Chem.* **1994**, *33*, 5113−5121.
(23) Bradley, D. C.; Mehrotra, R. C.; Gaur, D. P. *Metal Alkoxides*; Academic Press: London, 1987.
(24) Herrman, W. A.; Huber, N. W.; Runte, O. *Angew. Chem.* **1995**, *107*, 2371−2390.
(25) Valeria, G. M.; Olga, Yu. V.; Volodymyr, N. K.; Brian, W. S.; Dante, G. *New. J. Chem.* **2001**, *25*, 685−689.
(26) Ali, M.; Ray, A.; Sheldrick, S. W.; Mayer-Figge, H.; Gaoc, S.; Sahmesd, I. A. *New J. Chem.* **2004**, *28*, 412−417.
(27) Dominguez-Vera, M. J.; Camara, F.; Moreno, M. J.; Isac-Garcia, J.; Colacio, E. *Inorg. Chim. Acta* **2000**, *306*, 137−141.
(28) En-Qing, G.; Dai-Zheng, L.; Zong-Hui, J.; Shi-Ping, Y. *Polyhedron* **2001**, *20*, 923−927.
(29) Nesterov, S. D.; Makhankova, G. V.; Vassilyeva, Y. O.; Kokozay, N. V.; Kovbasyuk, A. L.; Skelton, W. B.; Jezierska, J. *Inorg. Chem.* **2004**, *43*, 7868−7876.
(30) Jin-Kui, T.; Shu-Feng, S.; Li-Ya, W.; Dai-Zheng, L.; Zong-Hui, J.; Shi-Ping, Y.; Cheng, P.; Liu, X. *Inorg. Chem. Commun.* **2002**, *5*, 1012−1015.
(31) Kessler, G. V.; Gohil, S.; Kritikos, M.; Korsak, N. O.; Knyazeva, E. E.; Moskovskaya, F. I.; Romanovsky, V. B. *Polyhedron* **2001**, *20*, 915−922.
(32) (a) Tahir, A. A.; Molloy, K. C.; Mazhar, M.; Kociok-Köhn, G.; Hamid, M.; Dastgir, S. *Inorg. Chem.* **2005**, *44*, 9207−92012. (b) Ribas, J.; Monfort, M.; Costa, R.; Solans, X. *Inorg. Chem.* **1993**, *32*, 695−699.
(33) El Fallah, M. S.; Rentschler, E.; Caneschi, A.; Sessoli, R.; Gatteschi, D. *Inorg. Chem.* **1996**, *35*, 3723−3724.
(34) Fleeting, K. A.; O'Brien, P.; Jones, A. C.; Ostway, D. J.; White, A. J. P.; Williams, D. J. *J. Chem. Soc., Dalton Trans.* **1999**, *16*, 2853−2859.

characterization of complexes **1**, **2**, and **3**, as well as the subsequent use of **2** and **3** as precursors for the deposition of thin films of $(Cu_{0.3}Co_{0.7})Co_2O_4$/CuO and $Ni_{0.95}Cu_{0.05}O$/CuO, respectively.

Experimental Section

All manipulations were carried out under an atmosphere of dry argon using Schlenk and glovebox techniques. Solvents were rigorously dried with sodium metal/benzophenone. $Co(acac)_2 \cdot xH_2O$, $Ni(acac)_2 \cdot xH_2O$, and lithium metal were purchased from Aldrich. All other reagents were purchased from Fluka. Elemental analysis was performed using a CHN analyzer LECO model CHNS-932. FAB mass spectra were measured on a JMS-HX-1100 spectrometer (JEOL, Japan). FT-IR spectra were recorded with a Bio-Rad Excalibur FT-IR model FTs 300MX spectrometer from KBr disks, and magnetic measurements were made using a commercial vibrating-sample magnetometer (VSM) model BHV-50 from Perkin Denshi Co., Ltd., Japan.

The controlled thermal analysis of the complexes was studied using a Perkin-Elmer thermogravimetric analyzer TGA7 with a computer interface. The measurements were carried out in an alumina crucible.

Scanning electron microscopy (SEM) was carried out using a JEOL JSM-5910 scanning electron microscope with a beryllium window. Metallic elemental ratios were recorded on an EDX analyzer Inca 200 from Oxford Instruments, U.K. XRD peak patterns of the powder were collected using a PANanalytical, X'Pert PRO diffractometer with Cu Kα radiation.

Single-crystal diffraction data for the mixed chloro−iodo derivative of **1** and for **2** were collected on a Bruker AXS SMART APEX CCD diffractometer at 100(2) K using monochromatic Mo Kα radiation with an ω-scan technique. The unit cell was determined using SAINT+, and the data were corrected for absorption using SADABS.[35]

The diffraction data of complex **3** were collected using a Nonius Kappa image-plate diffractometer at 150(2) K using monochromatic Mo Kα radiation. Using ϕ and ω scans we colleted 406 images at 1.5° increments.[36] The unit cell was determined, and the reflections were integrated and scaled with the HKL Denzo-Scalepack suite of programs,[37] and the data were corrected for absorption using Sortav.[38]

The structures of complexes **1** and **2** were solved by direct methods and refined by full-matrix least squares against F^2 with all reflections, using SHELXTL 6.10.[39] Structure **3** was solved by direct methods using SIR97[40] and refined by full-matrix least squares against F^2 using SHELXL97.[41] Reflections −1 0 3 and 1 2 3 were omitted. For all three compounds, refinement of an extinction coefficient was found to be insignificant. All non-hydrogen atoms were refined anisotropically.

Table 1. Growth Conditions for the Deposition of Mixed-Metal Oxide Thin Films from **2** and **3**

precursor concentration	0.2 g/25 mL (toluene)
carrier gas (N_2) flow rate (cm^3/min)	25
sample solution injection (mL/min)	0.25
furnace temp	450 °C
substrate	soda glass
deposition time	1.5 h

The mixed chloro−iodo derivative of **1** crystallizes with a disordered molecule of toluene in the asymmetric part of the unit cell. The occupancy ratio for the two orientations is 0.631(8):0.369(8). The toluene carbon atoms were restrained to be isotropic within a standard deviation of 0.1. Three of the four independent chlorine atoms showed a small contribution of disorder with iodine. All chlorine and iodine atoms were restrained to have the same anisotropic displacement parameters, and all Cu−Cl, as well as all Cu−I, distances were restrained to be each identical within a standard deviation of 0.02. The Cl/I occupancy ratios were found to be 0.908(1):0.092(1), 0.946(1):0.054(1), and 0.915(1):0.0885(1). The absolute structure factor for **1** refined to 0.022(8).

For the complexes **2** and **3**, the hydroxyl hydrogen atoms were located in the difference density Fourier map and were refined with an isotropic displacement parameter 1.2 times that of the adjacent oxygen atom. The O−H distances were restrained to be 0.82 Å for complex **2** and 0.89 Å for complex **3**. All other hydrogen atoms were placed in calculated positions and were refined with an isotropic displacement parameter 1.2 (CH and CH_2) or 1.5 (CH_3) times that of the adjacent carbon atom.

Complexes **2** and **3** are isostructural, and for both structures, significant voids are found in the unit cell, mainly localized in the center and at the corners of the unit cell around crystallographic inversion centers. The volumes of the voids are 90 and 69 $Å^3$ for complexes **2** and **3**, respectively. The difference electron density within these voids indicates the presence of solvent, and the spatial distribution is reminiscent of disordered toluene (the solvent used for crystallization). A tentative refinement, based on this assumption, resulted in occupancies of less than 10%, and the refinements were not stable. For the final refinements, the solvent was ignored, resulting in only minor increases in *R* values. Additional crystal data and experimental details for **1**, **2**, and **3** are listed in Table 2.

Synthesis of $[Cu(dmae)Cl]_4$ (1). The tetrameric *N*,*N*-dimethylaminoethanolato copper(II) chloride, $[Cu(dmae)Cl]_4$ (**1**), was synthesized following a modified literature procedure.[42] A solution of 0.05 g (7.20 mmol) of lithium in 15 mL of methanol was treated with a solution of 0.97 g (7.20 mmol) of copper(II) chloride in 15 mL of methanol to give a green suspension. After filtration, the solid was washed three times with 5 mL of methanol and dried under vacuum to give "(MeO)CuCl". The addition of 10 mL of toluene gave a green suspension, which became a dark green solution after treatment with 0.64 g (7.2 mmol) of *N*,*N*-dimethylaminoethanol. The reaction mixture was stirred for 10 min and evaporated to dryness under vacuum to give a green powder of $[Cu(dmae)Cl]_4$. Yield: 94%. mp: 131 °C. Anal. Calcd for $C_{16}H_{40}N_4O_4Cl_4Cu_4$: C, 25.66; H, 5.34; N, 7.48; Found: C, 25.52; H, 5.10; N, 7.52%. IR (cm^{-1}): 2966m, 2896w, 2893s, 2871s, 1465s, 1383m, 1343m, 1262s, 1060s, 1017m, 946s, 897s, 801s, 627s, 513m, 464s, 422s. FAB-MS: *m*/*z* (positive mode) Calcd (found) not observed, $[M]^+$; 645.98 (645), $[M - CuCl - 2H]^+$; 552.91 (553), $[M - (dmae)3Cl]^+$; 517.9 (517), $[M\text{-}(dmae)4Cl]^+$; 460.81

(35) *SAINT*, version 6.45; Bruker AXS Inc.: Madison, WI, 1997−2003.
(36) *Enraf-Nonius Collect Software*; Nonius BV: Delft, The Netherlands, 1997−2000.
(37) Otwinowski, Z.; Minor, W. *Methods in Enzymology*, 276; Carter, C. W., Jr., Sweet, R. M., Eds.; Academic Press: New York, 1997; pp 307−326.
(38) Blessing, R. H. *Acta Crystallogr.* **1995**, *A51*, 33−38.
(39) (a) *SMART for WNT/2000*, version 5.628; Bruker AXS Inc.: Madison, WI, 1997−2002. (b) *SHELXTL*, version 6.10; Bruker AXS Inc.: Madison, WI, 2000.
(40) For SIR97, see: Altomare, A.; Burla, M. C.; Camalli, M.; Cascarano, G. L.; Giacovazzo, C.; Guagliardi, A.; Moliterni, A. G. G.; Polidori, G.; Spagna, R. J. *Appl. Cryst.* **1999**, *32*, 115−119.
(41) Sheldrick, G. M. *SHELXL97, Program for Crystal Structure Analysis*, release 97-2; Institut für Anorganische Chemie der Universität: Göttingen, Germany, 1998.
(42) Anwander, R.; Munck, F. C.; Priermeier, T.; Scherer, W.; Runte, O.; Herrmann, W. A. *Inorg. Chem.* **1997**, *36*, 3545−3552.

Table 2. Crystal Data and Structure Refinement for Compounds **1**, **2**, and **3**

	1	2	3
empirical formula	$C_{23}H_{48}Cl_{3.77}Cu_4I_{0.23}N_4O_4$	$C_{26}H_{56}Cl_4Co_2Cu_4N_4O_{10}$	$C_{26}H_{56}Cl_4Cu_4N_4Ni_2O_{10}$
fw	861.78	1099.56	1098.12
solvent	toulene	toluene	toluene
cryst habit, color	plate, green	block, black	hexagon, green
temp	100(2) K	100(2) K	150(2) K
cryst syst	orthorhombic	monoclinic	monoclinic
space group	$Pna2_1$	$P2_1/n$	$P2_1/n$
unit cell dimensions	$a = 10.9840(12)$ Å	$a = 10.5625(8)$ Å	$a = 10.5830(2)$ Å
	$b = 27.250(3)$ Å	$b = 10.6274(8)$ Å	$b = 10.6460(2)$ Å
	$c = 11.1182(12)$ Å	$c = 19.7117(14)$ Å	$c = 19.6120(4)$ Å
		$\beta = 98.0950(10)°$	$\beta = 98.0630(10)°$
vol	3327.8(6) Å^3	2190.6(3) Å^3	2187.77(7) Å^3
Z	4	2	2
density (calcd)	1.720	1.662	1.667
absorption coeff	3.073	2.939	3.045
$F(000)$	1753.3	1112	1120
cryst size	0.43 × 0.35 × 0.07 mm^3	0.48 × 0.33 × 0.22 mm^3	0.10 × 0.10 × 0.03 mm^3
θ range	1.98−28.28°	2.08−28.28°	3.02−25.02°
index ranges	$-14 \le h \le 14$	$-14 \le h \le 11$	$-12 \le h \le 11$
	$-36 \le k \le 36$	$-14 \le k \le 14$	$-12 \le k \le 12$
	$-14 \le l \le 14$	$-26 \le l \le 26$	$-23 \le l \le 23$,
reflns collected	33 036	18 166	31 237
independent reflns	8235	5398	3854
abs correction	multiscan	multiscan	multiscan
max. and min. transm	0.810 and 0.421	0.526 and 0.332	0.9142 and 0.7505
data/restraints/params	8235/94/402	5398/1/236	3854/1/236
GOF on F^2	1.030	1.052	1.117
Final R indices [$I>2\sigma(I)$]	R1 = 0.0271, wR2 = 0.0647	R1 = 0.0255, wR2 = 0.0678	R1 = 0.0358, wR2 = 0.0663
R indices (all data)	0.0285, wR2 = 0.0653	R1 = 0.0281, wR2 = 0.0694	R1 = 0.0492, wR2 = 0.0700
largest diff. peak and hole	1.022 and −0.686 e Å^{-3}	0.726 and −0.386 e Å^{-3}	0.419 and −0.459 e Å^{-3}

(461), [M − 2(dmaeH)3Cl]$^+$; 369.72 (369) [M/2 − 4H]$^+$; 334.95 (333), [M/2 − 4H − Cl]$^+$; 276.07 (277), [M/4 + dmaeH]$^+$; 241.10 (241), [M/4 + dmae + 2H]$^+$; 186.0(186), [M/4]$^+$; 151.0 (151) [M/4 − Cl]$^+$. TGA: 109−214 °C (17.91 wt % loss), 214−800 °C (residue of 34.2%).

X-ray structural data for **1** was collected using a single crystal of a derivative with about 5.8% of the chlorine atoms replaced with iodine, which was found to be isotypic with the powder of **1** by comparison of the calculated powder pattern with that collected for crude **1** (Supporting Information). This mixed chloro−iodo compound was synthesized as an accidental side product of the reaction of $[Cu(dmae)Cl]_4$ with CdI_2 and was not otherwise characterized.

Synthesis of $Co_2(acac)_2(\mu\text{-}OH)_2Cu_4(dmae)_4Cl_4$ (2). One gram (3.89 mmol) of hydrated $Co(acac)_2{\cdot}xH_2O$ was added to a solution of 1.45 g (1.93 mmol) of $[Cu(dmae)Cl]_4$ (**1**) in 20 mL of toluene at room temperature. After the mixture was stirred for 5 h, the excess of $Co(acac)_2{\cdot}xH_2O$ was removed by filtration through a cannula. The reaction mixture was evaporated to dryness under vacuum, and the solid was redissolved in 7 mL of toluene to give a 65% yield of black crystals after 10 days at −10 °C. mp: 162 °C. The analysis of the resulting product resembled that for $Co_2(acac)_2(\mu\text{-}OH)_2Cu_4(dmae)_4Cl_4$, as determined by X-ray crystallography. Anal. Calcd for $C_{26}H_{56}N_4O_{10}Cl_4Co_2Cu_4$: C, 28.37; H, 5.13; N, 5.09. Found: C, 29.12; H, 5.10; N, 4.48%. IR (cm^{-1}): 3434br, 2963w, 2905w, 1578w, 1527w, 1413w, 1355w, 1263m, 1185w, 1071w, 1020m, 941m, 900m, 785s, 658m, 611m, 522m, 454s, 318w, 284s. FAB-MS: *m*/*z* (positive mode) calcd (found) 824.60 (825), [M − $Cu(dmae)_2Cl]^+$; 725.64 (725) [M − $Cu_2(dmae)_2Cl_2]^+$; 549.78 (553), [M/2]$^+$; 461.78 (461), [M/2 − dmae]$^+$; 402.85 (402) [M/2 − Co(dmae)]$^+$; 367.397 (369), [M/2 − Co(dmae)Cl]$^+$; 339.03 (342), [M/2 − CuCo(dmae)]$^+$; 277.93 (277), $[Co(acac)(dmae)(O)_2]^+$; 245.93 (244), [Co(acac)(dmae)]$^+$; 186.96 (185), [Cu(dmae)Cl]$^+$; 178.93 (177), $[Co(dmae)(O)_2]^+$; 157.93 (157), [Co(acac)]$^+$. TGA: 70−128 °C (17.65 wt % loss), 128−195 °C (13.46 wt % loss), 195−430 °C (residue 40.95%).

Synthesis of $Ni_2(acac)_2(\mu\text{-}OH)_2Cu_4(dmae)_4Cl_4$ (3). A solution of 0.50 g (0.67 mmol) of $[Cu(dmae)Cl]_4$ in 15 mL of toluene was transferred into a suspension of 0.34 g (1.33 mmol) of $Ni(acac)_2{\cdot}xH_2O$ in 10 mL of warm toluene. The reaction mixture was stirred at 80 °C for 2 h and was allowed to cool. Filtration through a cannula gave a clear dark green solution, which was concentrated under vacuum and crystallized by slow evaporation of the solvent through a septum to give a yield of 60% of **3** as a crystalline product. mp: 184 °C. Anal. Calcd for $C_{26}H_{56}N_4O_{10}Cl_4Ni_2Cu_4$: C, 28.45; H, 5.1; N, 5.1. Found: C, 29.12; H, 4.7; N, 5.8%. IR (cm^{-1}): 3428br, 2970w, 1581s, 1527w, 1399s, 1266w, 1188w, 1063w, 1019s, 940w, 783s, 613w, 455s, 319w, 283w. FAB-MS: *m*/*z* (positive mode) calcd (found) 946.62 (946), [M − Cu(dmae)]$^+$; 823.12 (823) [M − $Cu(dmae)_2Cl]^+$; 724.2 (723), [M − $Cu_2(dmae)_2Cl_2]^+$; 608.2 (608), [M − $Cu_2(acac)(OH)(dmae)_2Cl_2]^+$; 549.06 (553), [M/2]$^+$; 461.06 (461), [M/2 − dmae]$^+$; 402.35 (402) [M/2 − Ni(dmae)]$^+$; 366.97 (369), [M/2 − Ni(dmae)Cl]$^+$; 338.81 (341), [M/2 − CuNi(dmae)]$^+$; 277.71 (277), $[Ni(acac)(dmae)(O)_2]^+$; 245.71 (245), [Ni(acac)(dmae)]$^+$; 186.96 (185), [Cu(dmae)Cl]$^+$; 178.22 (177), $[Ni(dmae)(O)_2]^+$; 157.71 (156), [Ni(acac)]$^+$. TGA: 65−131 °C (17.65 wt % loss); 131−190 °C (13.20 wt % loss); 190−430 °C (residue of 39.80%).

Deposition of Thin Films. Mixed-metal oxide thin films were prepared on a soda glass substrate using an ultrasonic nebulizer to generate an aerosol as described elsewhere.[32a] The 1.5 × 4 cm soda glass substrate slides were positioned horizontally in a Pyrex glass tube in a furnace fitted with an aerosol generator assembly. Nitrogen gas and sample solution flow was manually controlled. Parameters for the growth of thin films are listed in Table 1.

Results and Discussion

Multifunctional ligands, such as aminoalkoxides, are a general tool to strengthen the interaction between the components of heterobimetallic species, and thus they would

be promising precursors for MOCVD and related applications. The limited use of metal alkoxides in this field can be mainly attributed to the fact that metal alkoxides often exist as μ-alkoxide-bridged oligomeric clusters which badly affect MOCVD requirements such as high volatility and a large temperature window between evaporation and thermal decomposition.

We have extensively explored the use of aminoalkoxides, β-diketonates, and carboxylates of two different metals for the preparation of heterobimetallic complexes in which chelating or bridging ligands can coordinate to the second metal. The use of multifunctional ligands allows each metal to achieve coordinative saturation from the available ligand set and minimizes the extent to which molecules must oligomerize to achieve the same result. In general, this approach will maximize the volatility or solubility of a complex, both attractive properties in CVD technology. We, therefore, have developed single-source precursors for the synthesis of mixed-metal oxides of copper with cobalt or nickel for the production of thin metal-oxide films for technological applications.

The synthetic procedures used in the synthesis of these heterobimetallic complexes are generally simple and involve mixing of the reactants in the proper molar ratios. Thus complexes $Co_2(acac)_2(\mu\text{-}OH)_2Cu_4(dmae)_4Cl_4$ (**2**) and $Ni_2(acac)_2(\mu\text{-}OH)_2Cu_4(dmae)_4Cl_4$ (**3**) were prepared in yields of more than 60% by reacting appropriate amounts of tetrameric *N*,*N*-dimethylaminoethanolato copper(II) chloride (**1**) with acetylacetonates of Co(II) and Ni(II) as shown in eq 1. Magnetic susceptibility measurement suggest that both the complexes are field-dependent paramagnetic.[43] The complexes are soluble in common organic solvents such as toluene, tetrahydrofuran, and alcohols and are stable in air under normal conditions.

$$2M(acac)_2{\cdot}xH_2O + [Cu(dmae)Cl]_4 \rightarrow M_2(acac)_2(\mu\text{-}OH)_2Cu_4(dmae)_4Cl_4 + 2\ acacH \quad (1)$$
$$M = Co\ (\mathbf{2}),\ Ni\ (\mathbf{3})$$

Complexes **1**, **2**, and **3** have been characterized by melting point, elemental analysis, FT-IR, mass spectrometry, and thermogravimetric analysis. Complex **1** is sensitive toward decomposition in solution, and all attempts to recrystallize it in solvents such as MeOH, EtOH, $CHCl_3$, toluene, and THF under various conditions resulted in a change of color from dark to light green and yielded only amorphous and ill-defined solids. The crude material was thus not further purified but used for the next steps as received from the reaction mixture. However, a derivative of **1** with ~5.7% of the chlorine atoms exchanged by iodine, synthesized as an unintended side product in the reaction of $[Cu(dmae)Cl]_4$ with cadmium iodide CdI_2 in toluene at ambient temperature, did form single crystals suitable for X-ray structural analysis which were found to be isotypic with the powder of **1** by comparison of the calculated powder pattern with that collected for crude **1** (Supporting Information). The green

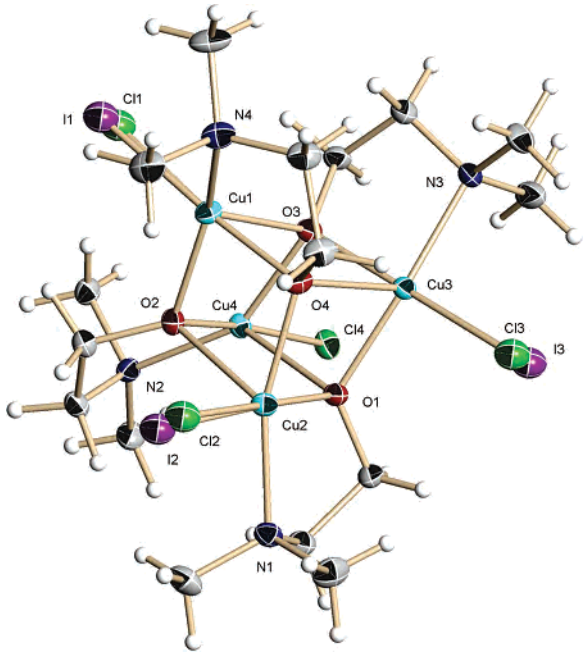

Figure 1. ORTEP plot of the mixed chloro−iodo derivative of **1**. The toluene solvate molecule and carbon and hydrogen labels have been omitted for clarity. Thermal ellipsoids are at the 50% level.

Table 3. Selected Metrical Data for $C_{23}H_{48}Cl_{3.77}Cu_4I_{0.23}N_4O_4$ (**1**)

bond distance (Å)		bond angles (deg)	
Cl(1)−Cu(1)	2.2612(13)	O(4)−Cu(1)−O(2)	86.18(8)
Cl(2)−Cu(2)	2.2352(12)	O(4)−Cu(1)−N(4)	84.61(9)
Cl(3)−Cu(3)	2.2619(15)	O(2)−Cu(1)−N(4)	151.91(9)
Cl(4)−Cu(4)	2.2479(7)	O(4)−Cu(1)−Cl(1)	172.93(7)
Cu(1)−O(4)	1.958(2)	O(2)−Cu(1)−Cl(1)	95.63(7)
Cu(1)−O(2)	1.999(2)	N(4)−Cu(1)−Cl(1)	96.76(8)
Cu(1)−N(4)	2.045(2)	O(4)−Cu(1)−O(3)	78.39(8)
Cu(1)−O(3)	2.369(2)	O(2)−Cu(1)−O(3)	74.98(7)
Cu(1)−I(1)	2.414(4)	N(4)−Cu(1)−O(3)	128.50(9)
Cu(2)−O(1)	1.9540(19)	Cl(1)−Cu(1)−O(3)	95.45(6)
Cu(2)−O(4)	2.002(2)	O(4)−Cu(1)−I(1)	175.38(11)
Cu(2)−N(1)	2.050(2)	O(2)−Cu(1)−I(1)	98.40(11)
Cu(2)−O(2)	2.3847(19)	N(4)−Cu(1)−I(1)	91.03(11)
Cu(2)−I(2)	2.466(6)	Cl(1)−Cu(1)−I(1)	7.91(8)
Cu(3)−O(3)	1.9541(19)	O(1)−Cu(2)−O(2)	78.44(7)
Cu(3)−O(1)	1.974(2)	O(4)−Cu(2)−O(2)	75.52(7)
Cu(3)−N(3)	2.058(2)	O(1)−Cu(2)−I(2)	170.94(14)
Cu(3)−O(4)	2.368(2)	O(4)−Cu(2)−I(2)	101.22(14)
Cu(3)−I(3)	2.448(4)	O(3)−Cu(4)−O(1)	75.17(7)
Cu(4)−O(2)	1.9568(19)	O(3)−Cu(1)−I(1)	103.31(9)
Cu(4)−O(3)	1.988(2)	O(1)−Cu(2)−O(4)	85.39(8)
Cu(4)−N(2)	2.038(2)	N(3)−Cu(3)−O(4)	115.88(9)
Cu(4)−O(1)	2.3444(19)	N(1)−Cu(2)−I(2)	90.29(15)

crystals with the composition $C_{16}H_{40}N_4O_4Cl_{3.77}I_{0.23}Cu_4$ were found to crystallize in the orthorhombic space group $Pna2_1$, exhibiting the expected cubelike tetrameric copper complex (Figure 1), similar to that observed previously for $[Cu(deae)X]_4$ (X = Cl, Br; deae = *N*,*N*-diethylaminoethanolate).[44,45] Three of the four crystallographically independent halogen atoms were found to have a small contribution of iodine between 5.4(1) and 9.2(1)%. The FAB mass spectrum does not exhibit the molecular ion peak for the tetramer at $m/z = 748$, but the tetrameric nature of chloro complex (**1**)

(43) Yuen, T.; Lin, C. L.; Fu, A.; Li, J. *J. Appl. Phys.* **2002**, *91*, 7385−7387.

(44) Estes, E. D.; Hodgson, D. J. *Inorg. Chem.* **1975**, *14*, 334−338.

(45) Mergehenn, R.; Merz, L.; Haase, W. *J. Chem. Soc., Dalton Trans.* **1980**, 1703−1709.

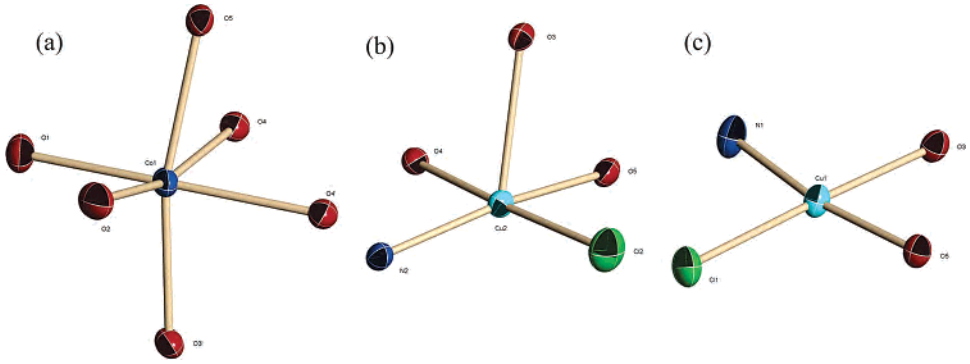

Figure 2. Geometric spheres of (a) octahedral Co, (b) square pyramidal Cu(1), and (c) square planar Cu(2) in **2**.

Table 4. Selected Metrical Data for $Co_2(acac)_2(\mu\text{-}OH)_2Cu_4(dmae)_4Cl_4$ (**2**)[a]

bond distances (Å)		bond angles (deg)	
Cl(1)−Cu(1)	2.2310(5)	O(3)−Cu(1)−O(5)	84.74(5)
Cl(2)−Cu(2)	2.2462(5)	O(3)−Cu(1)−N(1)	86.34(6)
Cu(1)−O(3)	1.9426(12)	O(5)−Cu(1)−N(1)	170.96(6)
Cu(1)−O(5)	1.9652(12)	O(3)−Cu(1)−Cl(1)	176.98(4)
Cu(1)−N(1)	2.0287(15)	O(5)−Cu(1)−Cl(1)	92.25(4)
Cu(1)−Cu(2)	2.8824(3)	O(3)−Cu(1)−O(1)	80.40(5)
Cu(2)−O(4)	1.9678(12)	O(4)−Cu(2)−O(5)	83.61(5)
Cu(2)−O(5)	1.9833(13)	O(5)−Cu(2)−N(2)	164.28(6)
Cu(2)−N(2)	2.0081(16)	O(4)−Cu(2)−Cl(2)	176.20(4)
Co(1)−O(1)	2.0362(13)	O(2)−Co(1)−O(1)	89.44(6)
Co(1)−O(2)	2.0258(13)	O(2)−Co(1)−O(3)#1	96.85(5)
Co(1)−O(3)#1	2.0991(11)	O(2)−Co(1)−O(4)	167.25(5)
Co(1)−O(4)	2.1126(12)	O(3)#1−Co(1)−O(4)	95.88(5)
Co(1)−O(5)	2.1350 (12)	O(1)−Co(1)−O(4)#1	173.28(5)
		O(2)−Co(1)−O(5)	91.01(5)
		O(1)−Co(1)−O(5)	95.31(5)
		O(4)−Co(1)−O(5)	76.64(5)
		O(4)#1−Co(1)−O(5)	86.07(4)
		Cu(1)−O(5)−Cu(2)	93.97(5)
		Cu(1)−O(3)−Co(1)#1	121.42(6)
		Cu(2)−O(5)−Co(1)	93.97(5)

[a] Symmetry operation: $1 - x, 1 - y, -z$.

Table 5. Selected Metrical Data for $Ni_2(acac)_2(\mu\text{-}OH)_2Cu_4(dmae)_4Cl_4$ (**3**)[a]

bond distances (Å)		bond angles (deg)	
Ni(1)−O(1)	1.998(2)	O(3)−Cu(1)−O(5)	84.43(9)
Ni(1)−O(2)	1.992(2)	O(3)−Cu(1)−N(1)	86.32(11)
Ni(1)−O(3)	2.079(2)	O(5)−Cu(1)−N(1)	170.60(11)
Ni(1)−O(4′)#1	2.087(2)	O(5)−Cu(1)−Cl(1)	92.40(7)
Ni(1)−O(5)#1	2.098(2)	O(4)−Cu(2)−O(5)	83.38(9)
Cu(1)−O(3)	1.940(2)	O(5)−Cu(2)−N(2)	163.15(11)
Cu(1)−O(5)	1.966(2)	O(4)−Cu(2)−Cl(2)	175.86(7)
Cu(1)−N(1)	2.027(3)	N(2)−Cu(2)−Cl(2)	97.23(9)
Cu(1)−Cl(1)	2.2315(10)	O(5)−Cu(2)−O(3)	74.90(9)
Cu(2)−O(4)	1.964(2)	N(2)−Cu(2)−O(3)	116.77(10)
Cu(2)−O(5)	1.979(2)	O(2)−Ni(1)−O(1)	91.55(10)
Cu(2)−N(2)	2.007(3)	O(1)−Ni(1)−O(3)	95.86(10)
Cu(2)−Cl(2)	2.2460(10)	O(2)−Ni(1)−O(4)#1	169.13(9)
		O(1)−Ni(1)−O(4)#1	88.24(9)
		O(3)−Ni(1)−O(4)#1	94.89(9)
		O(2)−Ni(1)−O(5)#1	91.59(9)
		Cu(1)−O(3)Ni(1)	104.50(5)
		Cu(2)−O(5)−Co(1)	122.40(6)

[a] Symmetry operation: $1 - x, 1 - y, -z$.

was further confirmed by the presence of wide range of other ions derived from the fragmentation of the tetramer.

The chloro−iodo derivative of **1** has a cubanelike structure (Figure 1) with four copper and four oxygen atoms alternately arranged at the vertexes of the cube. Each copper atom is surrounded by five donor atoms, three oxygens, one halogen, and one nitrogen and has an irregular geometry best described as being between trigonal bipyramidal and square pyramidal. The oxygen atoms of the cube exhibit a distorted tetrahedral environment with three copper atoms and one methylene carbon substituent. The Cu−O bond distances (Table 2) range from 2.385(2) to 1.954(2) Å, which is comparable to other Cu−O bond distances reported in the literature.[46] The Cu−Cl bond distances are 2.262(2)−2.235(1) Å, and the Cu−N distances range from 2.058(2) to 2.038(2) Å.

Complexes **2** and **3** were fully characterized by elemental analysis, FT-IR spectroscopy, mass spectrometry, and magnetometery and their structures were established by single-crystal X-ray diffraction. Both complexes are isostructural with each other and crystallize in the monoclinic space group $P2_1/n$ with two molecules per unit cell. Each of the $M_2(acac)_2(\mu\text{-}OH)_2Cu_4(dmae)_4Cl_4$ molecules (M = Co, Ni) is located on a crystallographic inversion center. Selected bond lengths and angles are listed in Tables 3 and 4, and the molecular structures of **2** and **3** are displayed in Figures 3 and 4. The six metal atoms are linked together by six oxygen atoms, two of which are μ_3-OH bridging hydroxyl anions, and the other four oxygen atoms belong to the chelating/bridging dmae groups. The coordination sphere of the metal atoms in complexes **2** and **3** is further augmented by the acetylacetonate oxygen atoms and the nitrogen donors of the dmae ligands. The geometric environment of each metal center (Figure 2) will be discussed in detail below for the cobalt structure (Figure 3) and is compared to the nickel complex (Figure 4) where necessary.

Cu(1) has an almost square planar geometry with a CuO_2-NCl core, made up of a chloride group [Cl(1)], one chelating dmae group [N(1), O(3)], the oxygen atom of which is triply bridging between Cu(1), Cu(2) and the symmetry-dependent cobalt atom Co(1′), and an hydroxyl group [O(5)] bridging Cu(1), Cu(2), and the nonsymmetry-dependent cobalt atom Co(1). The coordination environment of Cu(1) is further augmented by a weak Cu···Cu interaction with copper atom Cu(2) with a metal−metal separation of 2.8824(3) Å.

Cu(2) has a nonmetal coordination number of five with a CuO_3NCl ligation set composed of one chloride group [Cl-

(46) Vaartstra, B. A.; Samucle, J. A.; Barash, E. H.; Mertin, T. D.; Streib, W. E.; Gasser, C.; Cautton, K. G. *J. Organomet. Chem.* **1993**, *449*, 191−201.

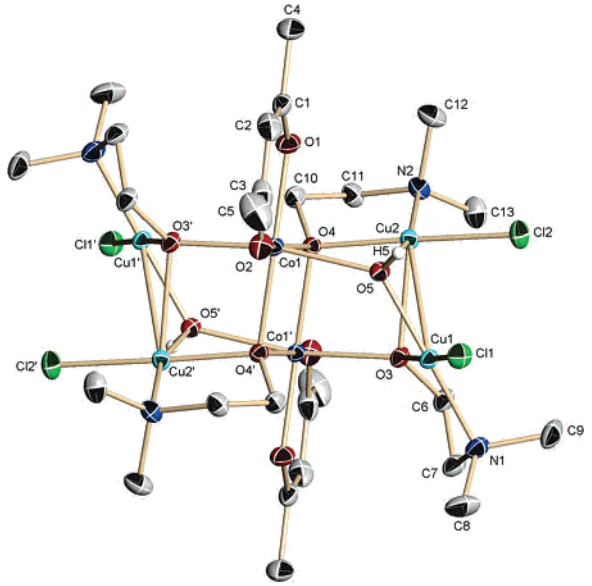

Figure 3. ORTEP drawing showing the molecular structure of $Co_2(acac)_2(\mu\text{-}OH)_2Cu_4(dmae)_4Cl_4$ (**2**); thermal ellipsoids are at the 30% level. Symmetry operation: $1-x, 1-y, -z$. All but the hydroxyl hydrogen atoms are omitted for clarity.

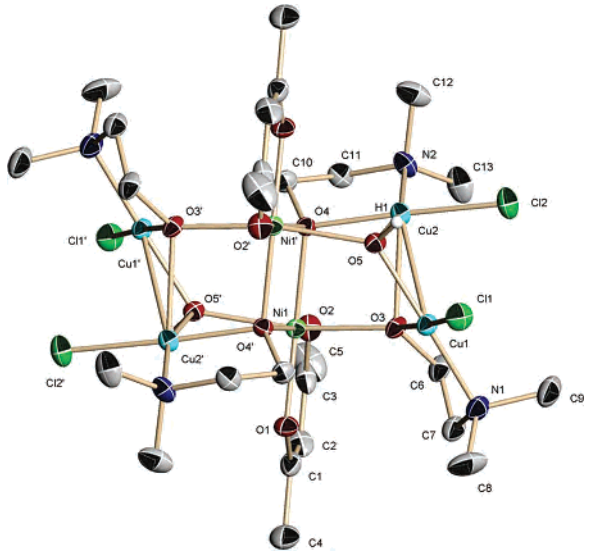

Figure 4. ORTEP drawing showing the molecular structure of $Ni_2(acac)_2(\mu\text{-}OH)_2Cu_4(dmae)_4Cl_4$ (**3**); thermal ellipsoids are at the 30% level. Symmetry operation: $1-x, 1-y, -z$. All hydrogen atoms, except for the hydroxyl hydrogen atoms, are omitted for clarity

(2)], a chelating/bridging dmae group [N(2), O(4)] (the oxygen of which acts as a bridge to both cobalt centers), an oxygen atom of the triply bridged dmae ligand [O(3)] connecting Cu(1) with Cu(2) and the Co(1) atom generated by the inversion center, and a doubly bridging hydroxyl anion [O(5)] also connecting Cu(1), Cu(2), and Co(1).

If the Cu···Cu interaction is omitted, the coordination environment of Cu(2) is distorted square pyramidal with an O(4)−Cu(2)−N(2) bite angle of 86.54(5)° (less than 90°) and an O(3)−Cu(2)−O(5) angle of 75.17(5)° (smaller than 90°). Also the copper−oxygen bond distance of Cu(2) to the apical oxygen atom O(3) is much longer (2.313(1) Å) than all other Cu−O bond lengths in complex **2**, which range from 1.943(1) for Cu(1)−O(3) to 1.983(1) for Cu(2)−O(5),

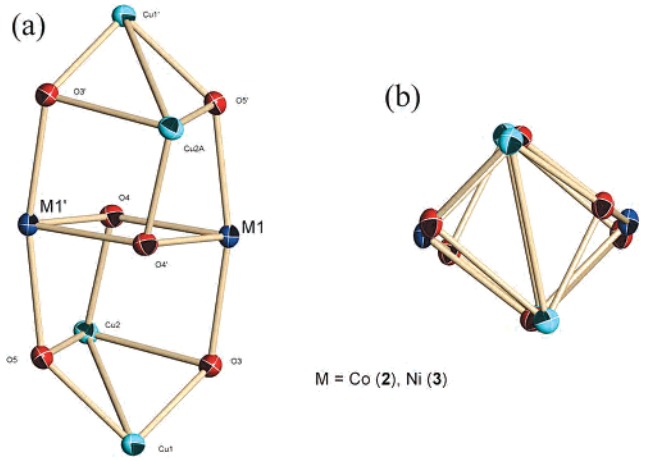

Figure 5. (a) Lateral and (b) top views of the core units of complexes **2** and **3**.

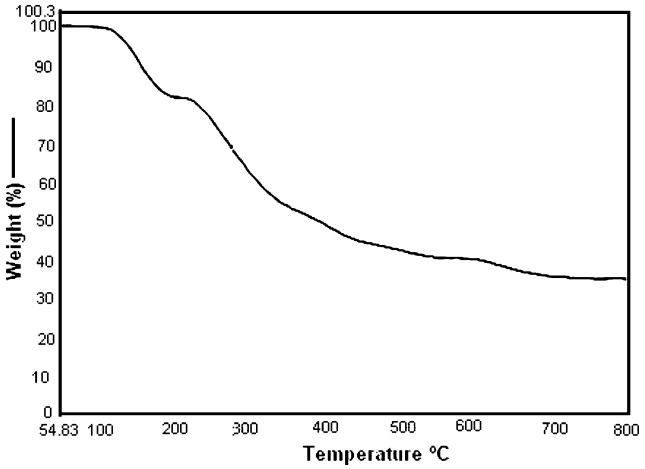

Figure 6. Thermogravimetric plot showing loss in weight with increase in temperature for complex **1**.

and they compare well with the sum of the ionic radii (1.92 Å).[46] The observed Cu−Cl bond lengths of 2.2310(5) and 2.2462(5) Å for Cu(1) and Cu(2), respectively, compare well with those of similar compounds.[47]

The cobalt (or nickel) centers have a coordination number of six with a coordination environment close to octahedral. Each cobalt atom is bonded to one chelating terminal acetylacetonate ligand in a η^2-manner [O(1), O(2)], three triply bridging dmae oxygen atoms [O(3′), O(4), O(4′)], and one triply bridging hydroxyl anion [O(5)]. O(4) connects both cobalt atoms with each other and with Cu(2); O(3) binds the cobalt atom Co(1′) to Cu(2) and Cu(1), and the hydroxyl anion O(5) connects Co(1) with the copper atoms Cu(1) and Cu(2). The observed Co−O distances range from 2.0258(13) to 2.1350(12) Å for Co(1)−O(1) and Co(1)−O(5), respectively, and are in general agreement with those found in similar complexes such as $[Co_2Ta_2(acac)_2(OMe)_{12}]$[48] or $[Co_4(acac)_4(OMe)_4(MeOH)_4]$[49] with only the triply bridged Co−O [O(3), O(5)] bond distances (2.099(1) and 2.135(1) Å) slightly longer than previously reported.[48]

(47) Shannon, R. D. *Acta Crystallogr.* **1976**, *A32*, 751−767.
(48) Werndrup, P.; Kessler, V. G. *J. Chem. Soc., Dalton Trans.* **2001**, *5*, 574−579.
(49) Bertrand, A. J.; Ginsberg, P. A.; Kaplan, I. R.; Kirkwood, E. C.; Martin, L. R.; Sherwood, C. R. *Inorg. Chem.* **1971**, *10*, 240−246.

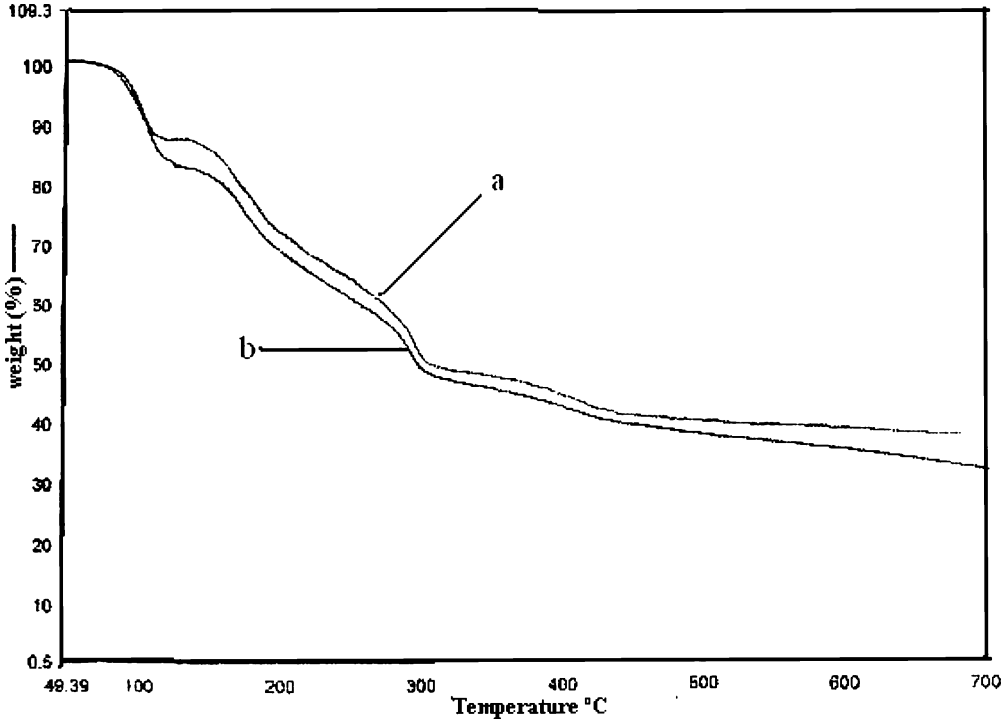

Figure 7. Thermogravimetric plot showing loss in weight with increase in temperature for complexes (a) **2** and (b) **3**.

The observed Ni−O_{acac} distances in complex **3** are 1.992(2) and 1.998(2) Å, which is in agreement with those found in $[Ni_2Ta_2(acac)_2(OMe)_{12}]$ but slightly shorter than the Co−O bonds of the cobalt complex **2**. The same is observed for the triply bridged Ni−O [O(3), O(4), O(5)] bond distances (2.079(2), 2.087(2), and 2.098(2) Å), which are also slightly shorter than those of complex (**2**), but similar to those in similar Ni complexes.[48]

A lateral and top view along the long axis of the core units of complex **2** or **3** is shown in Figure 5. The core units of complexes are composed of the two four-membered Cu_2O_2 square planes lying atop and below a similar four-membered M_2O_2 square (M = Co, Ni). The upper and lower squares are connected to the central one via the four μ-O of dmae and the two μ-OH groups, and the whole moiety thus has a $M_2Cu_4O_6$ unit as the core of the molecule.

Thermal Decomposition of Complexes 1, 2, and 3. The thermal behavior of precursor **1** and cage complexes **2** and **3** has been examined by thermogravimetric analysis, performed under an atmosphere of flowing nitrogen gas (25 mL/min). The thermograms of the three compounds, obtained with scanning rates of 10 °C/min, are shown in Figures 6 and 7, respectively. Complex **1** undergoes two major stages of weight loss upon heating. The first, occurring at 109−214 °C, is associated with a 17.91% weight loss. The second weight loss occurs at 214−800 °C, leaving a residue of 34.2%, corresponding well to copper metal (calcd as 33.9%). The TGA plots of complexes **2** and **3** show smooth thermal decomposition with several stages of weight loss to produce metal oxides. The fragmentation begins at 70 °C and is completed at 450 °C. The residual weight (40.95%) is slightly less, but close to the expected composition for $M_2Cu_4O_6$ (42.5% for both M = Co, Ni) indicating that the complexes have poor sublimation properties and decompose quantitatively to oxides. In these complexes, each metal center is coordinatively saturated by the oxygen atoms of the chelating acac and dmae ligands, thus eliminating the need for additional oxygen to form oxides. Thus, the new robust

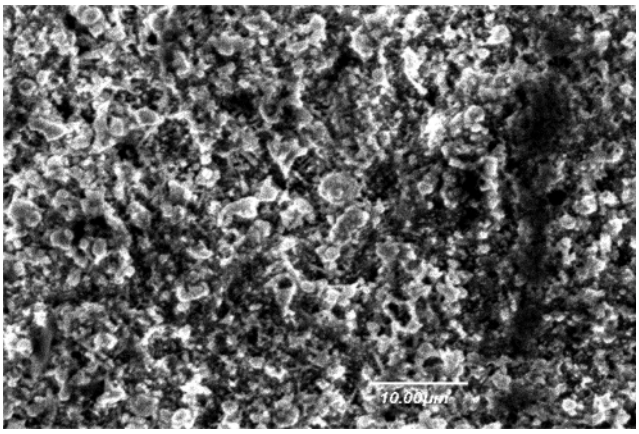

Figure 8. SEM micrograph of complex **2**.

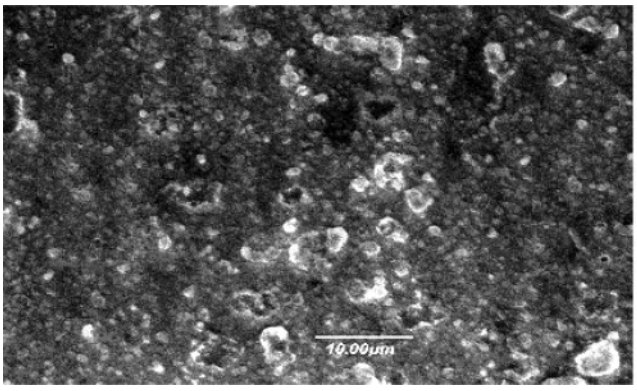

Figure 9. SEM micrograph of complex **3**.

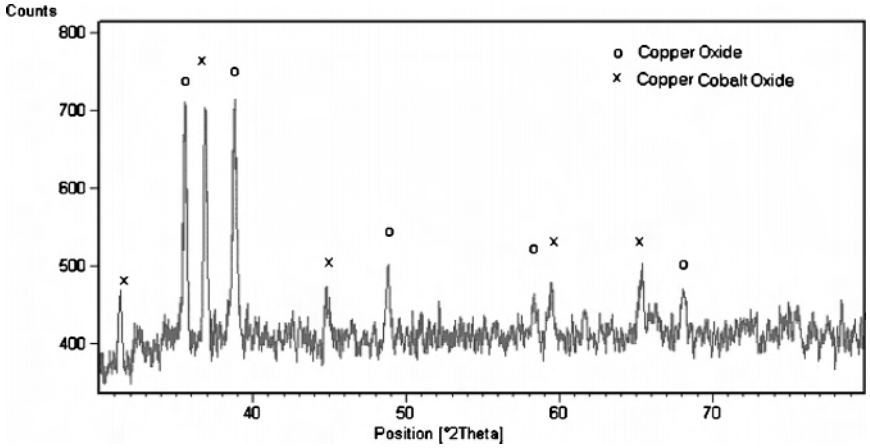

Figure 10. X-ray diffractogram of the oxide mixture obtained from complex **2**: x = $(Cu_{0.30}Co_{0.70})Co_2O_4$ [00-025-0270][50] and o = CuO [00-005-0661] (*syn*-tenurite).[52]

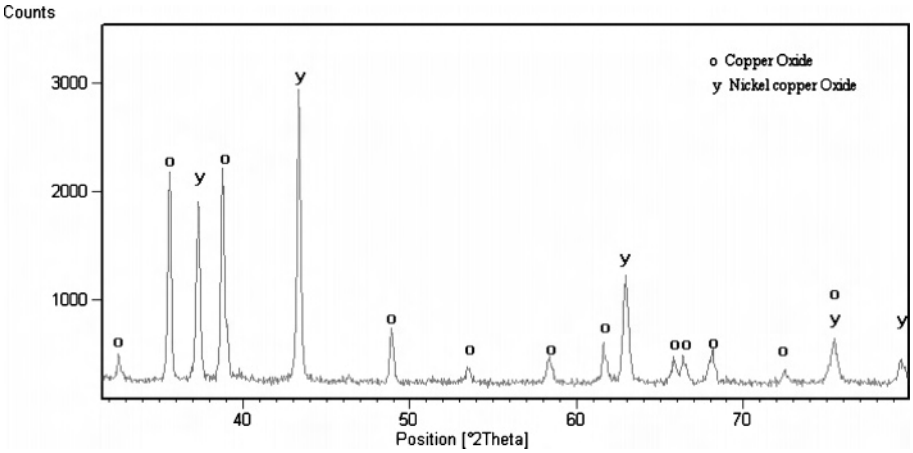

Figure 11. X-ray diffractogram of oxides obtained from complex **3**: y = $Ni_{0.95}Cu_{0.05}O$ [01-078-0644][51] and o = CuO [00-005-0661] (*syn*-tenurite).[52]

precursors are suitable for deposition of mixed-metal oxide films at the relatively low temperature of 450 °C.

FTIR spectra of the residues obtained after completion of the thermal gravimetric analysis of **1**, **2**, and **3** do not show any C═O stretching vibration bands, thus indicating the absence of any carbonate impurities. An absorption band observed at 530 cm^{-1} is in agreement with the presence of CuO as one of the decomposition products (eqs 2 and 3), which was also verified by XRD analysis of the residues (see below for details). Additional bands of medium intensity at 479, 339, and 229 cm^{-1} in the residue spectra of complexes **2** and **3** could not be assigned to any single metal oxide and thus might indicate the formation of mixed-metal oxides in addition to CuO. Thin films of the residues were prepared as described in the Experimental Section and were studied and characterized by SEM, EDX, and XRD. The films exhibit a good adhesion to the substrate and are stable toward air and moisture and qualify the "scotch tape test". They reflect light in multishaded colors depending upon the thickness of the deposited film. The scanning electron microscopy (SEM) image (Figure 8) of the oxide thin film deposited from complex **2** shows the film morphology with a spongy porous appearance having small crystallites evenly distributed with no preferred orientation, indicating the multiphase oxides. (See the discussion of the XRD powder data for more details of the nature of the multicomponent oxide mixture.) This observation supports our findings from XRD data which gives a clue of a multicomponent oxide mixture. The particles size ranges from 1.1 to 2.0 μm, and the grains have variable shapes without well-defined boundaries. The SEM image of oxide thin film deposited from complex **3** (Figure 9) shows a compact and smooth film morphology with homogeneously dispersed particles. The particle size ranges from 0.55 to 1.1 μm, and the grains are well defined with clear boundaries.

The energy dispersion X-ray analysis (EDX) analysis indicates a M/Cu (M = Co, Ni) ratio of close to 1:2 and the absence of nitrogen impurities from either the aminoalcohol or the carrier gas. Also no chlorine was detected by electron dispersion X-ray analysis (EDX) of the thin films, which is in agreement with the hypothesis that the presence of an electron-donor alkoxide group coordinated to the copper centers makes the Cu−Cl bond more susceptible for cleavage, thus resulting in the removal of chlorine. Removal of all impurities during the decomposition process leaving only the bridging oxygen atoms would ensure the formation of pure halide-free ceramic oxides, which was further supported by the XRD analysis.

The fingerprints of the powder X-ray diffractograms of the oxides obtained from the decomposition of complexes **2** and **3** (Figures 10 and 11) are in good agreement with the

reported data of $(Cu_{0.3}Co_{0.7})Co_2O_4$,[50] $Ni_{0.95}Cu_{0.05}O$,[51] and CuO.[52] Both of the oxide mixtures consist of highly crystalline phases with ratios of 29:71% for $(Cu_{0.3}Co_{0.7})Co_2O_4$/CuO and $Ni_{0.95}Cu_{0.05}O$/CuO, respectively. This observation suggests that the decomposition of complexes **2** and **3** proceeds according to the eqs 2 and 3.

$$27/2Co_2(acac)_2(\mu\text{-}OH)_2Cu_4(dmae)_4Cl_4 \xrightarrow{450\ ^\circ C} 10(Cu_{0.3}Co_{0.7})Co_2O_4 + 51CuO \quad (2)$$

$$19Ni_2(acac)_2(\mu\text{-}OH)_2Cu_4(dmae)_4Cl_4 \xrightarrow{450\ ^\circ C} 40Ni_{0.95}Cu_{0.05}O + 74CuO \quad (3)$$

The CuO found after both reactions is in the form of Tenorite,[52] having the monoclinic space group *C*2/*c*, with cell parameters of $a = 4.684$ Å, $b = 3.425$ Å, $c = 5.129$ Å, and $\gamma = 99.47°$. The Co−Cu oxide $(Cu_{0.3}Co_{0.7})Co_2O_4$ exhibits the cubic space group $Fd\bar{3}m$ with a unit cell edge of 8.074 Å, and the Ni−Cu oxide $Ni_{0.95}Cu_{0.05}O$ is also cubic with the space group $Fm\bar{3}m$ and an *a* axis of 4.1789 Å.

(50) ICDD powder diffraction database file card number [00-025-0270]. (b) Gallagher, McCarthy, Penn State University, University Park, PA, ICDD Grant-In-Aid, 1973.

(51) ICDD powder diffraction database file card number [01-078-0644]. (b) Schmahl, N. G.; Barthel, J.; Eikerling, G. F. *Z. Anorg. Allg. Chem.* **1964**, *332*, 230−237.

(52) ICDD powder diffraction database file card number [00-005-0661]. (b) Swanson, Tadge, *Natl. Bur. Stand. Circ.* (U.S.) **1953**, *539*, I 49.

Conclusion

The molecular structure design approach has permitted the high-yield synthesis of a new type of heterobimetallic cage complex, $M_2(acac)_2(\mu\text{-}OH)_2Cu_4(dmae)_4Cl_4$ (M = Co, Ni), as precursors to ceramic oxide materials. Structural and spectroscopic studies of these mixed-metal cages confirmed their individual identity and revealed their stability in solution, volatility, and suitability as precursors for nanocrystals of ceramic oxide phases. The increased solution stability makes **2** and **3** attractive precursors for preparation of films by chemical vapor deposition and nanoparticles ranging from 0.55 to 2.0 μm in size. Further studies of this and related systems can open new approaches to particles with controlled size and geometry for potential applications in electroceramic, catalysis, and sensor applications.

Acknowledgment. M.H., A.A.T., and M.M. acknowledge the Pakistan Science Foundation and Higher Education Commission, Islamabad, Pakistan, for financial support through Project PSF/R&D/C-QU/CHEM.(218) and "Merit Scholarship Scheme for PhD Studies in Science & Technology (200 Scholarships)". The Smart Apex diffractometer was funded by NSF Grant 0087210, by the Ohio Board of Regents Grant CAP-491, and by Youngstown State University.

Supporting Information Available: Crystallographic data in CIF format. This material is available free of charge via the Internet at http://pubs.acs.org.

IC060119U